# Energy shell structure of a single InAs/GaAs quantum dot with a spin-orbit interaction

M. Vachon,[1,2] S. Raymond,[1] A. Babinski,[3,4] J. Lapointe,[1] Z. Wasilewski,[1] and M. Potemski[1,3]
[1]*Institute for Microstructural Sciences, National Research Council of Canada, Ottawa, Ontario, Canada K1A 0R6*
[2]*Department of Physics, University of Ottawa, Ottawa, Ontario, Canada K1N 6N5*
[3]*Laboratoire des Champs Magnétiques Intenses, Centre National de la Recherche Scientifique, 25 Avenue des Martyrs, BP166, 38042 Grenoble, France*
[4]*Institute of Experimental Physics, University of Warsaw, Hoza 69, 00-681 Warsaw, Poland*
(Received 9 October 2008; revised manuscript received 13 March 2009; published 21 April 2009)

We study the evolution of the excited-state photoluminescence of a single self-assembled quantum dot as a function of applied magnetic field in a regime where the cyclotron energy is comparable to the confinement energy. As expected, we observe the splitting of the angular-momentum states following the Fock-Darwin scheme, but we also observe that each state further splits into a doublet which shows an unexpected evolution with increasing magnetic field. This behavior cannot be explained by a simple Zeeman spin splitting but is rather consistent with the observation of spin-orbit coupling where the spin of electrons is coupled with the envelope function orbital angular momentum. We show that the addition of this type of spin-orbit coupling to the single-particle Fock-Darwin model can account for the observed dependence. By comparison of our data with such a model, we derive a spin-orbit intensity of $[(3.9\pm0.3)\times10^{-9}$ eV cm$]^2$.

DOI: 10.1103/PhysRevB.79.165427 PACS number(s): 78.67.Hc, 73.21.La, 78.55.Cr, 81.07.Ta

The potential of quantum dot (QD) structures for nanotechnology applications has motivated considerable research on their fundamental properties. Both the charge and spin of carriers in QDs can be used as quantum bits in quantum information processing.[1] While electron-hole pairs (excitons) may offer easy coherent manipulation,[2] the spin state has a longer coherence time due to its insensitivity to electronic noise. Possible mechanisms to control and manipulate spin states include prominently the Datta-Das proposal for a spin-field-effect transistor[3] based on the Rashba spin-orbit (SO) interaction.[4] A more recent proposal exploits both the Rashba and Dresselhaus[5] coupling by tuning the Rashba SO intensity via gate voltages.[6] The basic understanding of QD properties is necessary in order to fully exploit the application potential of this type of devices. In particular, all SO effects must be measured and understood for full control of spin-flip mechanisms.

The energy shell structure of charge carriers in self-assembled QDs is approximately that of a particle confined in a two-dimensional parabolic potential,[7,8] and the harmonic-oscillator solutions are the Fock-Darwin (FD) states.[9] The evolution of the FD states in magnetic field shows a typical crisscross pattern, the FD spectrum, which is reproduced to a good approximation by the evolution of the QD photoluminescence (PL) emission peaks with magnetic field.[10] However, the inhomogeneously broadened (few tens of meV) spectra of QD ensembles prevent observation of more subtle spin-related effects (few meV). The QD ensemble broadening can be eliminated by isolating a single-quantum dot (SQD) using a nanohole patterned gold mask or by etching small mesas on the sample surface, and single QD studies were recently reported for magnetic fields up to 14 and 20 T.[11,12] In this paper we present excited-state PL of a SQD in magnetic fields up to 26 T, where emission lines associated with different spin configurations of the same FD state can be resolved. The evolution of each spin configuration is followed as a function of magnetic field, and we conclude that it is consistent with the observation of spin-orbit coupling between the particle spin and the envelope function orbital angular momentum.

The sample investigated in this work was grown by molecular-beam epitaxy on a semi-insulating GaAs substrate. The InAs QDs were formed by Stranski-Krastanow self-assembly,[13] and their height was controlled by an Indium flush at 5 nm.[14] The dots were grown on an undoped GaAs buffer layer with a nominal thickness of 205 nm for which the last 5 nm was deposited at the InAs growth temperature of 490 °C and capped with a 300 nm GaAs layer. Another uncapped QD layer was deposited on the sample under the same conditions for atomic force microscopy (AFM) measurements. The structure was annealed for 35 s at 850 °C in order to blueshift the emission into the sensitivity range of a charge coupled device (CCD) camera and to decrease the shell energy spacing.[15] The sample was subsequently covered with a nanohole pattern with 20/100-nm-thick Ti/Au film to optically isolate the dots. The emission spectrum was measured with the sample immersed in liquid helium ($T$=4.2 K) and subject to a magnetic field applied perpendicular to the plane of the dots (Faraday configuration). Fiber optics were used to deliver laser excitation ($\lambda$=514.5 nm) and for light collection, whereas piezodriven stages enabled precise positioning of a SQD below the fiber optics. Further details of the setup can be found in Ref. 11.

The surface QD layer provides an estimate to the QD density by way of AFM imaging. Together with PL mapping of the various sized nanoholes, we determine an approximate QD density of 3 dots/$\mu$m$^2$. The results presented in this paper are from a SQD contained in a $1\times1$ $\mu$m hole for which power-dependent PL spectra are shown in Fig. 1.[16] The lowest excitation power spectrum appears to be dominated by a single emission line from the $s$ shell. However, higher-resolution PL measurements of similar dots have shown that the ground-state emission is comprised of a few emission lines with a characteristic pattern.[17,18] From polarization-resolved experiments, the observed lines are attributed to neutral and singly charged exciton states. Increas-

 

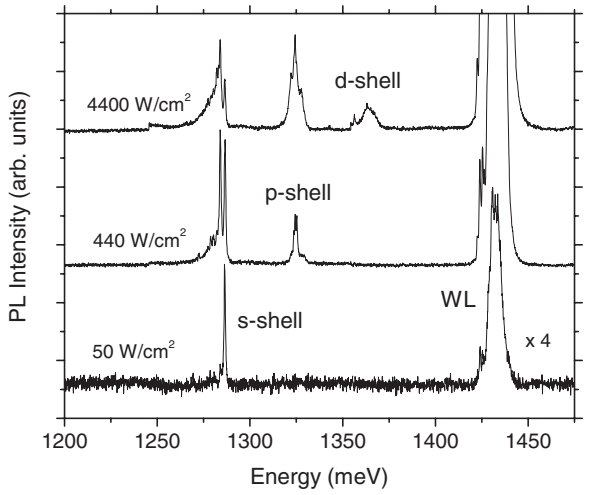


FIG. 1. Excitation power dependence of the PL spectrum from a SQD at zero magnetic field. As the power is increased, emission from higher energy shells appears in the spectra, and the wetting-layer signal gains intensity. The spectra are offset for clarity.

ing the power leads to shell-filling along with emission from the *p*-shell and subsequently the *d*-shell. Furthermore, there is a broadening effect as new emission lines appear at lower energies with respect to each shell, which we attribute to many-body effects.

The magnetophotoluminescence (MPL) measurements were taken at a relatively high excitation power in order to have the most intense signal from the *p*- and *d*-shells. The magnetic field evolution of the emission spectrum is presented in Fig. 2 in the form of a surface plot. The results resemble closely the simple FD spectrum with 1, 2, and 3 branches for the *s*-, *p*-, and *d*-shells, respectively, where each branch corresponds to a specific orbital angular-momentum channel. With increasing magnetic field, the lower angular-momentum states of the *f*- and *g*-shells emerge into the investigated energy range at ~6 and ~23 T, respectively. The spectrum evolution has the characteristic diamondlike level crossings of the FD spectrum, and the branches can unambiguously be assigned to specific excitonic FD states.[19] Several excitonic state crossings can be observed at ~9, ~16, and ~26 T with no apparent anticrossing behavior. Some deviations from the single-particle FD model are however observed. For example, the branches that belong to the same energy shell are not degenerate at zero field as predicted for FD states. Moreover, it is apparent that the zero and positive angular-momentum branches $L^e$ (Ref. 20) are composed of two emission lines that split progressively with increasing field. Conversely, the lower (negative angular momentum) branch of the *f*-shell is composed of a doublet which converges progressively as the magnetic field increases. For the lower branch of the *d*- and *p*-shells, a doublet is not directly seen, but the transition lines become narrower as the field increases, suggesting the presence of an unresolved doublet that converges with increasing field. A second derivative (data shown in Fig. 4) of the spectrum in Fig. 2 confirms the presence of a converging doublet for the lower branch of the *d*-shell.

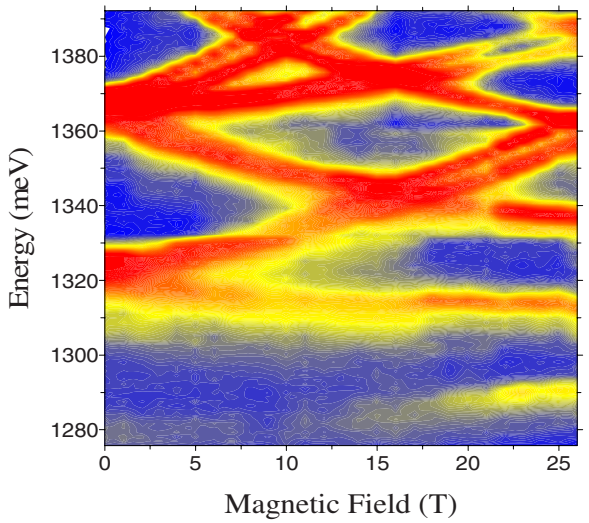


FIG. 2. (Color online) Surface plot of the SQD emission spectrum evolution in magnetic field. In order of increasing intensity, the emission is represented by blue, yellow, orange and red. The excitation intensity is ~38 kW/cm$^2$.

So far our discussion neglected carrier interactions, but in such a confined system of charged particles, interactions undoubtedly come into play. Since the doublets are separated by 5–10 meV throughout the magnetic field range and exchange energies are typically within a few meV, many-body effects should be considered as a possible reason for the presence of doublets. Many-body calculations show that the shifts due to exchange and correlation effects are usually toward lower energies.[8] As the excitation power is increased, the lower energy peak of the doublets would therefore be expected to appear after the higher energy peak. In view of that, power-dependent PL measurements were taken in static magnetic fields in order to study the effect of carrier population on the PL spectrum. In Fig. 3(a), the magnetic field is fixed at 6 T and the shell degeneracy has clearly been lifted as each PL peak can be assigned to a different orbital state. In particular, the *d*+ state is well isolated and it is apparent that it consists of a doublet. The doublet peaks appear in the PL spectrum following the filling of lower states, and their emission intensity increases gradually as the excitation power is increased. Moreover, the higher energy peak, which is very weak when the doublet first appears, becomes more intense with respect to the lower energy peak. The same behavior is observed for the *p*+ doublet at 22 T, as shown in Fig. 3(b). At the highest excitation power, the higher energy peak is more intense than the other doublet peak. This behavior is indicative of normal-state filling, which suggests that the doublets are not a manifestation of many-body effects but rather a manifestation of the two optically active spin configurations predicted by the single-particle picture. Finally, adding a simple Zeeman splitting to the FD model cannot explain the increased splitting of upper branches in magnetic field while lower branches show reduced splitting.

All of the above observations can be explained by the addition of SO coupling to the FD model. Such modifications to the FD model were implemented by several authors in the past to study the transport properties of electrons through gated QDs.[21–25] We extend this to the case of exci-

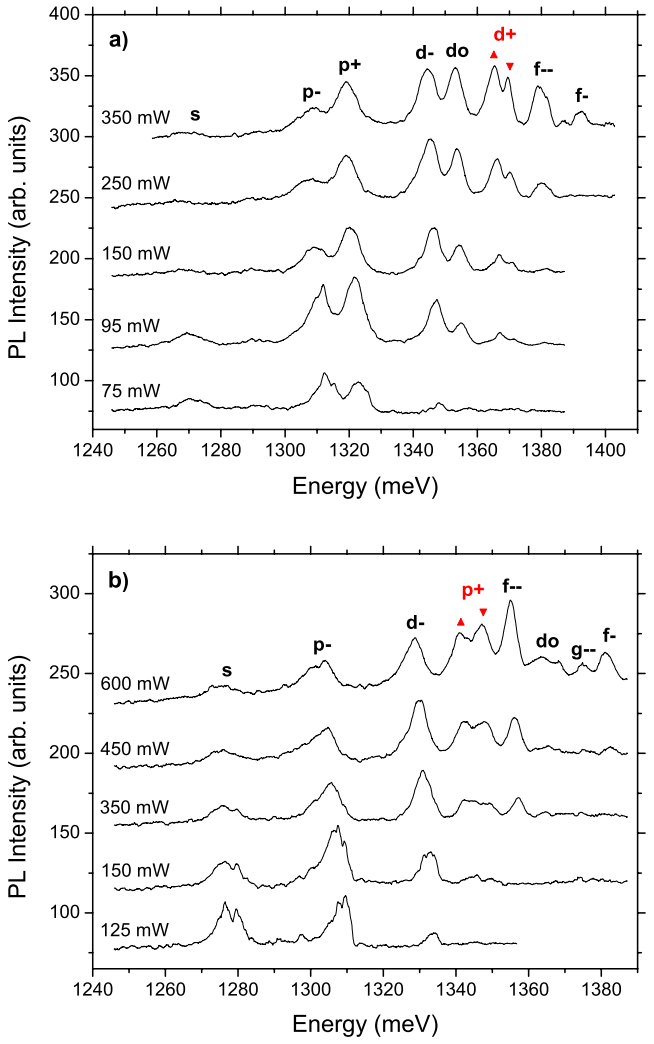


FIG. 3. (Color online) Power dependence of the PL from a SQD in a magnetic field fixed at (a) 6 and (b) 22 T. The doublet peaks appear in the PL spectrum following the filling of lower states. As the excitation power is increased, the higher energy peak becomes more intense with respect to the other doublet peak. The peaks have been denoted by arrows to symbolize their attribution to different spin states. However, it should be noted that the exact orientation of the spin states is not known.

tons in self-assembled dots to illustrate how SO coupling can explain our observations. For simplicity we work within the effective-mass approximation. We first consider a single-charged particle of effective-mass $m_\beta^*$ confined in the $xy$ plane by the potential $V^\beta(r)$; where $\beta$ stands for electron or hole. The dot shape can be accounted for by considering an anisotropic lateral potential,

$$V^\beta(\vec{r}) = \tfrac{1}{2}m_\beta^*(\omega_{\beta x}^2 x^2 + \omega_{\beta y}^2 y^2). \tag{1}$$

In a perpendicular magnetic field $B_z$, the single-particle Hamiltonian contains the confinement energy, the Rashba and Dresselhaus SO terms, and the Zeeman energy. When the confinement energy is much greater than the SO terms, one may use unitary transformations yielding an effective diagonal SO term to obtain analytical solutions.[26] The details are given in Refs. 21 and 26 and only the solution is presented here. The eigenvalues for each spin $\eta$ depend on the number of quanta in each oscillator,

$$E^\beta_{N_1N_2\eta} = \pm\left[\left(N_1+\tfrac{1}{2}\right)\hbar\Omega^\beta_{1\eta} + \left(N_2+\tfrac{1}{2}\right)\hbar\Omega^\beta_{2\eta}\right] + \tfrac{1}{2}s_\eta g^*_\beta \mu_B B_Z, \tag{2}$$

where $\pm$ has a positive (negative) sign for electrons (holes), $g^*_\beta$ is the bulklike effective $g$ factor, $\mu_B$ is the Bohr magneton, and $s_\eta = \pm 1$ for $\eta = \uparrow, \downarrow$. The frequencies $\Omega^\beta_{k\eta}$ of the two $(k=1,2)$ decoupled oscillators are

$$\Omega^\beta_{k\eta} = \tfrac{1}{\sqrt{2}}[\omega^2_{\beta x} + \omega^2_{\beta y} + \omega^2_{\beta\eta c} \pm \sqrt{(\omega^2_{\beta x} + \omega^2_{\beta y} + \omega^2_{\beta\eta c})^2 - 4\omega^2_{\beta x}\omega^2_{\beta y}}]^{1/2}, \tag{3}$$

where the upper (lower) sign in $\pm$ corresponds to $k=1(2)$. The cyclotron frequency has been renormalized to include the SO coupling,

$$\omega_{\beta\eta c} = \frac{eB_z}{m^*_\beta} + \lambda^\beta_{\mathrm{SO}}\frac{2m^*_\beta}{\hbar^3}s^\beta_\eta, \tag{4}$$

where the SO coupling constant $\lambda^\beta_{\mathrm{SO}}$ quantifies the total SO strength, including Dresselhaus and Rashba contributions.

Thus, we have obtained a set of states of the form $|N_1N_2\eta\rangle$ for both electrons and holes, with $N_k$ $(k=1,2)$ representing a number of renormalized oscillator quanta. It is interesting to note that for $\lambda^\beta_{\mathrm{SO}}=0$ and $\omega_{\beta x}=\omega_{\beta y}$, the above solution reduces to the traditional FD states where $\Omega_1=\Omega_+$ and $\Omega_2=\Omega_-$.[10] Now one must build the set of optically allowed transitions in order to compare with the experiment. In the case of pure FD states, dipole-allowed transitions couple electron and hole states with the same quantum numbers but opposite spins. Since the SO energies (few meV) are small compared to the lateral confinement energies (tens of meV), the same selection rules should apply to a good approximation. The excitonic $(X)$ spectrum is thus built from the difference between electron and hole energies $E^e_{N_1N_2\eta=\uparrow,\downarrow} - E^h_{N_1N_2\eta=\downarrow,\uparrow}$. An offset energy $E_0$ comprising the QD material energy gap and the vertical confinement energy must also be added to the exciton recombination energy. For an exciton state $|N_1N_2\eta\rangle$, where $\eta$ is defined as the electron spin, the emission energy is

$$E^X_{N_1N_2\eta} = E_0 + \left(N_1+\tfrac{1}{2}\right)\hbar\Omega^X_{1\eta} + \left(N_2+\tfrac{1}{2}\right)\hbar\Omega^X_{2\eta} + \tfrac{1}{2}s_\eta(g^*_e + g^*_h)\mu_B B_Z, \tag{5}$$

$$\Omega^X_{k\uparrow} = \Omega^e_{k\uparrow} + \Omega^h_{k\downarrow}; \quad \Omega^X_{k\downarrow} = \Omega^e_{k\downarrow} + \Omega^h_{k\uparrow}. \tag{6}$$

Figure 4 compares the calculated energies (lines) to the experimental results (circles), where experimental peak positions were extracted using a second derivative algorithm. In a strained InAs/GaAs QD, the electron effective mass becomes close to the electron mass in GaAs and we accordingly use the value $m^*_e=0.067m_e$ in the model.[7,27,28] Empirical pseudopotential and *ab initio* local-density calculations predict a heavy-hole mass of $m^*_h=0.590m_e$.[29] In a bulk semiconductor, the effective $g$ factor of the electron is altered from the free-electron value of $g\cong 2$ as a result of spin-orbit coupling related to the atomistic part of the wave function.

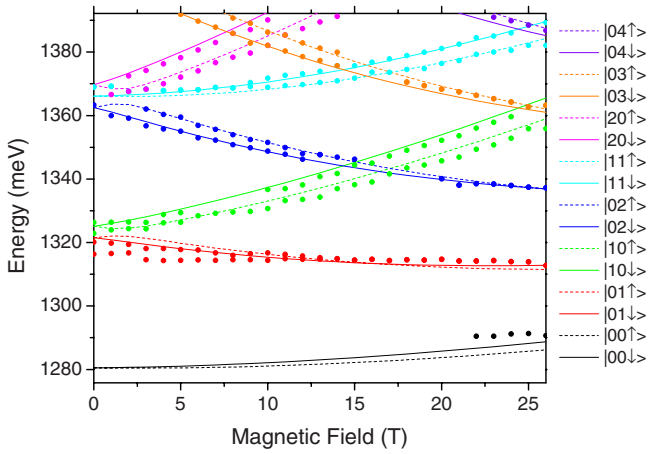


FIG. 4. (Color online) Comparison of calculated emission energies for our spin-orbit Fock-Darwin model (solid lines) compared with experimental peak positions (solid points). The parameters used include an anisotropic lateral potential with $\delta$=0.95, confinement potential strength of 35.4 meV and 7.4 meV for the electron and hole, respectively, and $E_0$=1238 meV. The model includes the Zeeman spin splitting and SO coupling.

These bulklike effects are included in the formula for conduction-band $g$ factor,[30]

$$g = 2 - \frac{2E_p\Delta_{\mathrm{SO}}}{3E_g(E_g + \Delta_{\mathrm{SO}})}, \tag{7}$$

where $\Delta_{\mathrm{SO}}$ is the spin-orbit splitting defining the energy difference between heavy and split-off hole states, $E_p = 2\langle S|P_x|X\rangle^2/m_e$ is the Kane energy involving the momentum matrix element between the $s$-like conduction band and $p$-like valence band, and $E_g$ is the band-gap energy including the vertical confinement energy. For InAs material,[28] the parameters are $\Delta_{\mathrm{SO}}$=0.39 eV, $E_p$=21.5 eV, and $E_g$=1.243 eV for the measured dot. This gives an effective electron $g$ factor $g_e^*$=−0.75 in the dot material. For holes in self-assembled dots, it was recently shown using a tight-binding approach that the hole $g$ factor is close to zero ($g_h^* \approx 0$).[31] Moreover, for the type of QDs studied here, we expect the dot anisotropy ratio $\delta = \omega_{\beta y}/\omega_{\beta x}$ to be close to unity, and from the ground- and excited-state peak positions at zero field, one can obtain good guesses for the offset energy as well as the electron and hole potential strength $\hbar(\omega_{\beta x} + \omega_{\beta y})/2$. The only fitting parameters left are the electron and hole SO intensities. We find that the best fit to our data is obtained when neglecting the hole spin-orbit coupling in comparison with that of electrons. This empirical observation is in agreement with theoretical results of other authors. Bulaev and Loss[32] argued that for flat QDs the SO coupling of electrons is stronger than that of heavy holes. Sheng *et al.*[31] found that the hole spin in InGaAs/GaAs QDs is "frozen" along the growth axis. This precludes efficient coupling of the "hole spin" with envelope function degrees of freedom.

A value of $\lambda_{\mathrm{SO}}^e = (3.9 \times 10^{-9}$ eV cm$)^2$ is obtained by minimizing the divergence between experimental and calculated results. This value is comparable to what is measured or predicted for InAs QWs.[33] However, in the QDs this value is achieved without external applied electric fields (i.e., no gates) or charge density. The difference lies in the strain distribution of the InAs material inside the QD which is different from that of a QW, and the asymmetry of the QD potential in the vertical direction, a result of the asymmetric shape and/or material composition inside the QD, whereas the asymmetry encountered for QWs in the literature stems from electric fields due to the presence of space charges in a 2DEG. The QD material strain affects the bulk inversion asymmetry (Dresselhaus), while asymmetry of the QD potential is related to the structural inversion asymmetry (Rashba). Our results do not allow us to discriminate between the two contributions, and the spin-orbit intensity obtained is a measure of the combined effect of both contributions. We expect that the measured value can change from dot to dot due to variations in composition, strain field, and structural shape. This would be consistent with the findings of Fry *et al.*[34] who indicated that a reversal of the permanent dipole in the vertical direction of QDs can be observed if the gradient of composition and the thickness of the QDs are varied. Further study should reveal more on this particular topic.

Although the SO coupling alone will introduce a zero field splitting of the different $L^e$ states within the same energy shell, we found that a small size anisotropy effect of 5% ($\delta$=0.95) was needed to explain the observed separations. If the SO coupling is too high, the evolution of the state splittings with magnetic field cannot be reproduced accurately. The strength of the SO coupling compatible with our data produces a zero-field splitting of ~2.6 meV between $p$-shell states. This is too small to explain the width of emission lines observed at zero field. As a result, a dot anisotropy that accounts for roughly 25% of the zero-field splitting of ~3.6 meV was introduced. However, a single-exciton model with size anisotropy and Zeeman spin splitting alone cannot reproduce the observed results. The evolution of each doublet depends on the envelope function angular momentum of that state. The branches with zero or positive angular-momentum $L^e$ have a doublet separation that gradually increases with field. Moreover, the separation is greater for states with more angular momentum and for same angular-momentum states that are in higher energy shells. For the negative angular-momentum branches, the lines appear to be initially separated and they converge together with increasing field until they form a unique peak. Furthermore, the separation depends on the orbital state. For fields between 5 and 10 T, the separation is greater as the angular-momentum $L^e$ is more negative. The dependence of the splitting on orbital state is a clear indication of SO interaction in the dot.

In general, there is good agreement between experimental and theoretical results. The main features of the MPL measurements are captured by the single-exciton model. The most important discrepancy occurs in the $s$-shell emission with the experimental peak maxima being at higher energies than the calculated results. However, the $s$-shell signal is relatively weak and broadened toward lower energies, which might explain the disagreement. The calculated spin splitting in the $s$ shell (2.5 meV at 26 T) is larger than what is observed in low excitation power measurements (0.6 meV at 26

T). We were not able to account for this discrepancy within the framework of our model. The bulklike effects on the effective $g$ factor have been accounted for in the value of $g_e^*$ used in the model. In the QD, the effective $g$ factor is further modified by SO coupling. The SO intensity determined from our calculations is therefore a measure of this added SO coupling. The SO interaction modifies the precessional frequency of the dot particles from the Larmor frequency $\omega_L = |g|\mu_B B/\hbar$ to a different value depending on the orbital state of the particles. The altered precessional energy is equal to the difference between the spin-up and spin-down particle energies for a given angular-momentum state, and its magnetic field dependence is related to the SO intensity. The effective $g$-factor values reported in the literature are determined from this altered precessional energy which will depend on dot size and shape[17,35] as a consequence of variation in SO intensity.

Although the above single-particle model successfully describes our experimental results, a more precise description should be obtained by the inclusion of many-body effects which should give more insight on the role of exchange and correlations. However, from the success of our single-particle model, one can infer that the SO interaction is a higher-order effect, while many-body effects are of an equivalent or lesser order, which vary more slowly with magnetic field than the SO coupling.

We consider that the largest parameter uncertainty in the theoretical model originates from the effective excitonic $g$ factor $g_{\mathrm{exc}}^* = g_e^* + g_h^*$ in the bulklike dot material. In order to determine an uncertainty on the SO intensity, we use the boundary values of 0 and −5 found in Ref. 35 for QDs of different geometry emitting at the same ground-state energy. We thus obtain $\lambda_{\mathrm{SO}} = [(3.9 \pm 0.3) \times 10^{-9}\ \mathrm{eV\ cm}]^2$.

In conclusion, we have shown that the emission spectrum of a SQD in magnetic field resembles the FD spectrum. By including SO coupling, Zeeman spin splitting, and dot-size anisotropy to the FD model, the calculated energies are in good agreement with the experimental results. The occurrence of doublets and their evolution as a function of increasing magnetic field is consistent with the observation of SO interaction in the dot. By comparing experimental data with a single-particle model, and neglecting the SO coupling of holes, a SO intensity of $(3.9 \times 10^{-9}\ \mathrm{eV\ cm})^2$ was deduced for electrons confined in our single self-assembled QD. We believe that this is the first experimental quantitative estimate for this coupling constant in self-assembled QDs.

This work was supported by EC under Grant No. RITA-CT-2003-505474. S.R. and M.V. would like to acknowledge NSERC for their support. A.B. would like to acknowledge the support of the EC Grant No. MTKD-CT-2005-029671. We are deeply grateful to our colleagues P. Hawrylak, M. Korkusinski, and S. J. Cheng for their invaluable comments.

[1] D. Bouwmeester, A. Ekert, and A. Zeilinger, *The Physics of Quantum Information* (Springer, Berlin, 2000); *Semiconductor Spintronics and Quantum Computation*, edited by D. D. Awschalom, D. Loss, and N. Samarth (Springer, Berlin, 2002).

[2] A. Zrenner, E. Beham, S. Stufler, F. Findeis, M. Bichler, and G. Abstreiter, Nature (London) **418**, 612 (2002); T. H. Stievater, Xiaoqin Li D. G., Steel, D. Gammon, D. S. Katzer, D. Park, C. Piermarocchi, and L. J. Sham, Phys. Rev. Lett. **87**, 133603 (2001); H. Htoon, T. Takagahara, D. Kulik, O. Baklenov, A. L. Holmes, Jr., and C. K. Shih, *ibid.* **88**, 087401 (2002).

[3] S. Datta and B. Das, Appl. Phys. Lett. **56**, 665 (1990).

[4] Y. A. Bychkov and E. I. Rashba, J. Phys. C **17**, 6039 (1984).

[5] G. Dresselhaus, Phys. Rev. **100**, 580 (1955).

[6] J. Schliemann, J. C. Egues, and D. Loss, Phys. Rev. Lett. **90**, 146801 (2003).

[7] A. Wojs, P. Hawrylak, S. Fafard, and L. Jacak, Phys. Rev. B **54**, 5604 (1996).

[8] P. Hawrylak, Phys. Rev. B **60**, 5597 (1999).

[9] V. Fock, Z. Phys. **47**, 446 (1928); C. G. Darwin, Proc. Cambridge Philos. Soc. **27**, 86 (1931).

[10] S. Raymond, S. Studenikin, A. Sachrajda, Z. Wasilewski, S. J. Cheng, W. Sheng, P. Hawrylak, A. Babinski, M. Potemski, G. Ortner, and M. Bayer, Phys. Rev. Lett. **92**, 187402 (2004).

[11] A. Babinski, M. Potemski, S. Raymond, J. Lapointe, and Z. R. Wasilewski, Phys. Rev. B **74**, 155301 (2006).

[12] A. Babinski, M. Potemski, S. Raymond, J. Lapointe, and Z. R. Wasilewski, Phys. Status Solidi **3**, 3748 (2006).

[13] D. J. Eaglesham and M. Cerullo, Phys. Rev. Lett. **64**, 1943 (1990); R. Leon and S. Fafard, Phys. Rev. B **58**, R1726 (1998).

[14] Z. R. Wasilewski, S. Fafard, and J. P. McCaffrey, J. Cryst. Growth **201-202**, 1131 (1999).

[15] S. Fafard and C. Ni. Allen, Appl. Phys. Lett. **75**, 2374 (1999).

[16] The authors note that the same experiment was performed on a different dot in the same sample, where the same experimental features are observed. The only variations are in the emission energy and the spacing of the energy shells, as could be expected for a dot of slightly different size and composition.

[17] A. Babinski, G. Ortner, S. Raymond, M. Potemski, M. Bayer, W. Sheng, P. Hawrylak, Z. Wasilewski, S. Fafard, and A. Forchel, Phys. Rev. B **74**, 075310 (2006).

[18] L. Landin, M. S. Miller, M.-E. Pistol, C. E. Pryor, and L. Samuelson, Science **280**, 262 (1998).

[19] For a definition of excitonic Fock-Darwin states, see S. Raymond, S. Studenikin, A. Sachrajda, Z. Wasilewski, S. J. Cheng, W. Sheng, P. Hawrylak, A. Babinski, M. Potemski, G. Ortner, and M. Bayer, in Proceedings—Electrochemical Society, Vol. PV 2004–13, pp. 23–38 (2005).

[20] For this portion of the discussion where we neglect carrier interactions and spin-orbit coupling, we refer to the orbital angular momentum of the electrons since they offer the dominant effects (confinement and cyclotron energy) due to their smaller effective mass.

[21] M. Valín-Rodríguez, A. Puente, and L. Serra, Phys. Rev. B **69**, 085306 (2004).

[22] M. Florescu and P. Hawrylak, Phys. Rev. B **73**, 045304 (2006).

[23] O. Voskoboynikov, C. P. Lee, and O. Tretyak, Phys. Rev. B **63**,

165306 (2001).
[24] I. L. Aleiner and Vladimir I. Fal'ko, Phys. Rev. Lett. **87**, 256801 (2001).
[25] J. Könemann, R. J. Haug, D. K. Maude, V. I. Fal'ko, and B. L. Altshuler, Phys. Rev. Lett. **94**, 226404 (2005).
[26] M. Valín-Rodríguez, A. Puente, L. Serra, and E. Lipparini, Phys. Rev. B **66**, 165302 (2002).
[27] D. Smirnov, S. Raymond, S. Studenikin, A. Babinski, J. Leotin, P. Frings, M. Potemski, and A. Sachrajda, Physica B **346-347**, 432 (2004).
[28] I. Vurgaftman, J. R. Meyer, and L. R. Ram-Mohan, J. Appl. Phys. **89**, 5815 (2001).
[29] M. A. Cusack, P. R. Briddon, and M. Jaros, Phys. Rev. B **56**, 4047 (1997).
[30] S. Zwerdling, B. Lax, L. M. Roth, and K. J. Button, Phys. Rev. **114**, 80 (1959); L. M. Roth, B. Lax, and S. Zwerdling, *ibid.* **114**, 90 (1959).
[31] W. Sheng and A. Babinski, Phys. Rev. B **75**, 033316 (2007).
[32] D. V. Bulaev and D. Loss, Phys. Rev. Lett. **95**, 076805 (2005).
[33] R. de Sousa and S. Das Sarma, Phys. Rev. B **68**, 155330 (2003); D. Grundler, Phys. Rev. Lett. **84**, 6074 (2000).
[34] P. W. Fry, I. E. Itskevich, D. J. Mowbray, M. S. Skolnick, J. J. Finley, J. A. Barker, E. P. O'Reilly, L. R. Wilson, I. A. Larkin, P. A. Maksym, M. Hopkinson, M. Al-Khafaji, J. P. R. David, A. G. Cullis, G. Hill, and J. C. Clark, Phys. Rev. Lett. **84**, 733 (2000).
[35] T. Nakaoka, T. Saito, J. Tatebayashi, and Y. Arakawa, Phys. Rev. B **70**, 235337 (2004).